THE JOURNAL OF BIOLOGICAL CHEMISTRY VOL. 285, NO. 18, pp. 13694–13703, April 30, 2010

Deficiency of Suppressor Enhancer Lin12 1 Like (SEL1L) in Mice Leads to Systemic Endoplasmic Reticulum Stress and Embryonic Lethality*[S]

Received for publication, November 25, 2009, and in revised form, March 1, 2010 Published, JBC Papers in Press, March 2, 2010, DOI 10.1074/jbc.M109.085340

Adam B. Francisco[‡], Rajni Singh[‡], Shuai Li[‡], Anish K. Vani[‡], Liu Yang[§], Robert J. Munroe[¶], Giuseppe Diaferia[**], Marina Cardano[‡‡], Ida Biunno[§§], Ling Qi[§], John C. Schimenti[¶], and Qiaoming Long[‡1]**

*From the [‡]Department of Animal Science and [§]Division of Nutritional Sciences, College of Agriculture and Life Sciences, and the [¶]Department of Biomedical Sciences, College of Veterinary Medicine, Cornell University, Ithaca, New York 14850, **BioRep, Via Fantoli 16/15, 20090 Milan, Italy, the [‡‡]Doctorate School of Molecular Medicine, University of Milan, 20090 Milan, Italy, and the [§§]Institute for Biomedical Technologies, National Research Council, Via Fratelli Cervi, 93, 20090 Segrate, Milan, Italy*

Stress in the endoplasmic reticulum (ER) plays an important causal role in the pathogenesis of several chronic diseases such as Alzheimer, Parkinson, and diabetes mellitus. Insight into the genetic determinants responsible for ER homeostasis will greatly facilitate the development of therapeutic strategies for the treatment of these debilitating diseases. Suppressor enhancer Lin12 1 like (SEL1L) is an ER membrane protein and was thought to be involved in the quality control of secreted proteins. Here we show that the mice homozygous mutant for SEL1L were embryonic lethal. Electron microscopy studies revealed a severely dilated ER in the fetal liver of mutant embryos, indicative of alteration in ER homeostasis. Consistent with this, several ER stress responsive genes were significantly up-regulated in the mutant embryos. Mouse embryonic fibroblast cells deficient in SEL1L exhibited activated unfolded protein response at the basal state, impaired ER-associated protein degradation, and reduced protein secretion. Furthermore, markedly increased apoptosis was observed in the forebrain and dorsal root ganglions of mutant embryos. Taken together, our results demonstrate an essential role for SEL1L in protein quality control during mouse embryonic development.

The endoplasmic reticulum (ER)[2] plays a critical role in the biosynthesis of proteins destined for the secretory pathway. Nearly all newly synthesized secreted or membrane-bound proteins must fold and assemble into their functional conformations in the ER before they are released into the post-ER compartments. Proteins that fail to or incorrectly undergo conformational maturation are retained in the ER and are eventually degraded through proteolysis (1). The protein folding/maturation process in the ER is both aided and monitored by ER chaperons and folding enzymes (2).

ER folding capacity and client protein load are precisely coupled to ensure ER homeostasis. Several cellular conditions, such as high demand for protein synthesis and secretion (3, 4), viral infection (5), deprivation of nutrients/oxygen (6, 7), and missense mutations affecting both client protein folding (8–11) and ER folding machinery function (2) enhance protein misfolding and cause accumulation of unfolded or misfolded proteins, leading to ER stress. Mammalian cells use several adaptive mechanisms, collectively known as the unfolded protein response (UPR), to cope with acute ER stress (12). Upon ER stress, translation is generally attenuated to reduce production of ER client proteins. Concomitantly, transcription of genes encoding ER chaperones and ER-associated degradation (ERAD) machinery is increased. Although up-regulation of ER chaperons enhance the ER folding/assembling capacity (13), increase of ERAD components ensures more efficient removal of terminally unfolded or misfolded proteins (14). These adaptive measures provide a multifaceted strategy to maintain ER homeostasis under temporary and reversible ER stress conditions.

The UPR is initiated by signal transducers, which are ER transmembrane proteins (15). Mammalian cells express three UPR signal transducers: inositol-requiring transmembrane kinase and endonuclease 1 (IRE1), protein kinase-like ER kinase (PERK), and activating transcription factor 6 (ATF6). All three transducers are maintained in an inactive state through interaction with the ER chaperone protein BiP (16). Upon ER stress, BiP is released from IRE1 and PERK to bind unfolded proteins, resulting in IRE1 and PERK undergoing homodimerization and activation (17). Activated IRE1 has endoribonuclease activity and cleaves 26 nucleotides from the mRNA encoding X-box-binding protein 1 (XBP1), causing a frameshift in the translation of XBP1 (18, 19). The spliced XBP1 (XBP1s) functions as a transcriptional activator for a large set of genes encoding ER chaperones and components of the ERAD and apoptosis pathways (20, 21). Activated PERK phosphorylates eukaryotic initiation factor 2α, which in turn leads to a general attenuation

* This work was supported by a grant from the College of Agricultural and Life Science, Cornell University (to Q. M. L.).

[S] The on-line version of this article (available at http://www.jbc.org) contains supplemental Fig. S1.

[1] To whom correspondence should be addressed: 321 Morrison Hall, Cornell University, Tower Road, Ithaca, NY 14850. Tel.: 607-254-5380; Fax: 607-255-9829; E-mail: ql39@cornell.edu.

[2] The abbreviations used are: ER, endoplasmic reticulum; UPR, unfolded protein response; ERAD, ER-associated degradation; TM, tunicamycin; TG, thapsigargin; Gluc, Gaussia luciferase; hpt, hours post-transfection; DM, deletion mutant; FL, full-length; IRE1, inositol-requiring transmembrane kinase and endonuclease 1; PERK, protein kinase-like ER kinase; ATF6, activating transcription factor 6; SEL1L, suppressor enhancer Lin12 1 like; GFP, green fluorescent protein; PBS, phosphate-buffered saline; RT, reverse transcription; MEF, mouse embryonic fibroblast; TUNEL, TdT-mediated dUTP nick-end labeling; E, embryonic; ES, embryonic stem; NHK, null Hong-Kong mutant; XBP1, X-box-binding protein 1.

of protein translation (22, 23). Release of BiP from membrane-bound ATF6 facilitates its translocation to the Golgi, where it is cleaved by Site-1 and Site-2 proteases (S1P and S2P) to free the cytosolic N terminus, a basic leucine zipper transcription factor (24). Activated ATF6 translocates to the nucleus where it binds to the ER stress responsive element in genes encoding ER chaperone proteins (25, 26).

SEL1L (suppressor enhancer Lin12 1 like) is a widely expressed ER membrane protein (type I) with a complex domain structure (27). Biochemical and molecular studies *in vitro* revealed that in eukaryotic cells SEL1L nucleates an ER membrane protein complex that is required for dislocation of unfolded or misfolded proteins from the ER lumen into the cytosol for degradation (28–33). *Sel1l* expression is inducible by ER stress and appeared to be controlled by ER-stress responsive transcription factors ATF6 and XBP1 (34). Several splicing isoforms of SEL1L have been identified and were shown to be involved in novel mechanisms of protein degradation or secretion (35). Together, these studies have underscored the importance of *Sel1l* in maintaining ER homeostasis in mammalian cells.

The developmental and physiological roles of *Sel1l* in vertebrates have not yet been determined. To characterize the *in vivo* functions of *Sel1l*, we have introduced a gene trap mutation into the *Sel1l* genomic locus. Analysis of the mutant embryos demonstrates that *Sel1l* is essential for embryonic survival. SEL1L deficiency results in impaired ERAD and protein secretion in mammalian cells. These molecular defects cause increased apoptosis in mutant embryos and hypersensitivity of embryonic cells to ER stress-inducing reagents. *Sel1l* thus plays a key role in maintaining ER homeostasis during vertebrate embryonic development.

MATERIALS AND METHODS

Mice—The *Sel1l* mutant mice were generated by microinjection of a gene-trapped mouse embryonic stem cell line, CA0017 (Sanger Institute Gene Trap Resource), into C57/BL6 blastocysts. The resulting chimeric male founders were backcrossed to C57BL/6 females to generate heterozygous ($Sel1l^{+/-}$) mice. $Sel1l^{+/-}$ mice were then intercrossed to generate homozygous $Sel1l^{-/-}$ embryos. Genotyping of all animals or embryos was done by PCR using the following primers: F1-Sel1l, 5′-TGGGACAGAGCGGGCTTGGAAT-3′; R1-Sel1l, 5′-CACCAGGAGTCAAAGGCATCACTG-3′; R-βGeo, 5′-ATTCAGGCTGCGCAACTGTTGGG-3′. All animal experiments were performed in accordance with the Cornell Animal Care and Use Guidelines.

Expression Plasmids—The Gaussia luciferase reporter plasmid was from New England Biolabs. The pNHK-GFP fusion expression plasmid was a kind gift from Dr. Nobuko Hosokawa of Kyoto University. The full-length (FL) and deletion mutant (DM) SEL1L-GFP fusion constructs were generated by PCR amplification of the corresponding *Sel1l* cDNA fragments followed by subcloning into the EcoRI and BamHI sites in pEGFP-N2 vector (Clontech). The PCR primers used to amplify the full-length and 5′ portion *Sel1l* cDNA fragments were: F2-Sel1l, 5′-GAATTCCGCCACCATGCAGGTCCGCGTCAGG-3′; R2-Sel1l, 5′-GGATCCtCTGTGGTGGCTGCTGCTC-3′; R3-Sel1l, 5′-GGATCCTAACTTGAACGCCTCTTCC-3′. The subcloned *Sel1l* cDNA fragments were verified by sequencing and the expression of fusion proteins were verified by GFP fluorescence microscopy in transfected HEK293 cells.

TUNEL Assay—Embryos were fixed in 4% paraformaldehyde in phosphate-buffered saline (PBS), processed, and paraffin-embedded using a standard procedure. Sections were cut at 5 μM and TUNEL assay was performed using the DeadEnd Colorimetric Apoptosis Detection System (Promega). Briefly, sections were rinsed 3 times with distilled H_2O, once in PBS, and permeabilized with 200 μg/ml of Proteinase K in PBS for 30 min. The permeabilized sections were incubated with equilibration buffer for 10 min at room temperature. DNA strand break labeling and colorization were performed as essentially recommended by the manufacturer. The TUNEL-stained tissue sections were counterstained lightly with hematoxylin, dehydrated, and mounted with Permount (Daigger).

Embryonic RNA Isolation and Quantitative RT-PCR—Total RNA was isolated from embryos of defined genotypes at E12.5 using the TRIzol RNA Isolation Kit (Invitrogen). For quantitative RT-PCR analysis, total RNA was treated with DNase I for 10 min and purified using the RNAqueous-Micro Kit (Ambion). First-strand cDNA was synthesized using SuperScript III Reverse Transcriptase (Invitrogen). Quantitative PCR was performed using Power SYBR Green PCR Master Mix on an ABI Prism 7000 Sequence Detection System (Applied Biosystems). Quantification and normalization of mRNA expression was performed essentially as described (36). Expression difference between wild-type and mutant cells was statistically analyzed by performing Student's *t* tests using the normalized mean value.

Embryonic Protein Isolation and Immunoblotting Analysis—Embryos from $Sel1l^{+/-}$ inter-crosses were dissected at E7.5 and lysed in a buffer containing 10 mM Tris-HCl (pH 7.4), 150 mM NaCl, 1% Nonidet P-40, protease inhibitors (Halt TM Protease Inhibitor Mixture EDTA-free, Pierce), 1 mM phenylmethylsulfonyl fluoride, 1 mM EDTA, and 1 mM sodium fluoride. The protein concentration of the embryonic lysates was determined by BCA assay (Thermo Fisher Scientific) and 12 μg of each lysate was resolved on 9% SDS-polyacrylamide gel, blotted to polyvinylidene difluoride, and then immunodecorated with specific antibodies: anti-SEL1L (37), anti-β-galactosidase (1:1000) (Chemicon International), anti-β-tubulin using standard procedures (43). Western blot hybridizations were performed using X-blot-100 chamber (Isenet.it) and proteins were detected using an ECL kit (Thermo Scientific) according to the manufacturer's specifications, and developed using the UVP Chemi Camera.

Establishment of $Sel1l^{+/+}$, $Sel1l^{+/-}$, and $Sel1l^{-/-}$ Mouse Embryonic Fibroblast (MEF) Cell Lines—MEFs with defined genotypes were prepared and cultured essentially as described with minor modifications (38). Briefly, females were sacrificed at day 12.5–13.5 of gestation. Embryos were decapitated and eviscerated and carcasses were homogenized. The homogenate was passed through a mesh to remove large tissue debris. The flow-through was plated on a gelatin-coated tissue culture plate and cultured in Dulbecco's modified Eagle's medium with 10% fetal bovine serum (Atlanta Biologicals).

Cells were split 1:3 every 2–3 days. To establish MEF cell lines, primary MEF cells of defined genotypes were maintained at 80–90% confluence in 10-cm dishes for two to three months.

Tunicamycin Treatment and Crystal Violet Assay—Tunicamycin (TM) treatment of MEF cells was performed essentially as described (39). TM stock was prepared in Me_2SO at ×1000 concentration (2 mg/ml) and held as single-use aliquots. MEF cells of defined genotypes (primary or cell lines) were plated into five 6-cm dishes at 2×10^5 cells per dish and allowed to rest overnight before application of stress. MEFs were then treated with 2 μg/ml of TM for 0, 1, 2, and 4 h. For untreated cells, Me_2SO alone was added to a final concentration of 0.1%. TM-treated MEFs were rinsed twice with PBS, trypsinized, re-plated into 10-cm dishes, and cultured for 5 days. Crystal violet staining was performed essentially as described (26). Briefly, MEFs in 10-cm dishes were rinsed with PBS and stained with 1 ml of 0.2% (w/v) crystal violet (Sigma) in 2% ethanol for 10 min at room temperature, washed three times with water, and dried. Stained MEFs were solubilized with 600 μl of 1% SDS, and absorbance of the resulting solution was measured at 570 nm. Relative cell viability was calculated as a percentage of absorbance of stressed cells relative to that of unstressed cells.

MEF Cell Transfection and Pulse-Chase Assay of NHK—All MEF cell transfections were done using polyethylenimine (Sigma). MEF cells of defined genotypes were seeded at a density of 0.5×10^6 cells/well in 6-well dishes. After an overnight rest, MEF cells were rinsed twice with PBS, once with Opti-MEM reduced serum medium (Invitrogen), and incubated for 12–16 h with 1 ml of Opti-MEM reduced serum medium containing 3 μg of expression plasmid encoding GFP-tagged NHK (for co-transfection, 3 μg of each expression plasmid was used) and 2 μl of polyethylenimine. Protein pulse-chase assay was performed as previously described (40). MEF cells were treated with 50 μg/ml of freshly prepared cycloheximide for 0, 1, 1.5, 3, 4.5, and 6 h. MEF cell lysates were prepared in 100 μl of Tris-buffered saline (pH 7.5) containing 1% Triton X-100 and protein concentrations were determined by bicinchoninic acid assay (BCA). For immunoblotting, 20 μg of each lysate was mixed with an equal volume of 2× sample buffer (100 mM Tris, 25% glycerol, 2% SDS, 0.01% bromphenol blue, 10% 2-mercaptoethanol), boiled for 5 min and loaded into a 9% gel for SDS-PAGE. Electrophoresis, blotting, and antibody probing were performed using standard procedures (41). Immunodetection was done using the Western blotting Luminol Reagent Kit (Origene) according to the manufacturer's specifications. GFP (Abcam) and tubulin (Cell Signaling) antibodies were used at 1:5,000 and 1:10,000, respectively). NHK-GFP and tubulin band intensities were quantified using the AlphaEase FC software on an AlphaImager 2200 imaging system. The NHK level in each treatment was normalized using the corresponding tubulin level. Relative NHK degradation was calculated as a percentage of the NHK level in non-treated cells. Experiments were performed three times and the data were expressed as the mean ± S.D. Statistical significance was considered as $p \leq 0.05$.

Gaussia Luciferase Assay—Gaussia luciferase assay was performed essentially as described (42). Briefly, MEF cells were grown to 60–70% confluence in 6-cm dishes and transfected with 7 μg of expression plasmid encoding Gaussia luciferase (Gluc) reporter (New England Biolabs). Conditioned medium of the transfected cells were sampled in triplicate at 12, 24, and 36 h post-transfection and mixed with an equal volume of freshly prepared 2× coelenterazine solution (Prolime Ltd./Nanolight). Gluc activity was measured at a wavelength of 470 μM for 10 s using a luminometer (Dynex). To measure intracellular Gluc activity, transfected MEF cells were washed 3 times with PBS and lysed in fresh culture medium through repeated freezing and thawing. Gluc activity in cell lysates was measured using the aforementioned luciferase assay protocol. Relative Gluc activity was calculated by normalizing to corresponding wild-type or mutant controls.

Transmission Electron Microscoping—*Sel1l*$^{+/+}$, *Sel1l*$^{+/-}$, and *Sel1l*$^{-/-}$ embryos were dissected at E12.5. The livers of these embryos were fixed in EMS Karnovsky's fixative mix (2% paraformaldehyde and 2.5% glutaraldehyde in 0.1 M phosphate buffer) for 1 h at room temperature. Specimen processing, sectioning, and transmission electron microscoping image acquisition were performed by the Electron Microscopy and Histology Core Facility, Department of Cell and Developmental Biology, Weill Cornell Medical College.

Statistical Analysis—Differences between groups were evaluated by performing two-tailed Student's *t* test and $p < 0.05$ is considered significant.

RESULTS

SEL1L Function Is Essential for Early Mouse Embryonic Development—*Sel1l* gene trap mice were generated using a commercially available embryonic stem (ES) cell clone, CA0017. This ES cell clone contains an exon trap (consisting of a splicing acceptor site and a β-galactosidase-neomycin fusion cassette) in intron 14 of *Sel1l*, as revealed by the rescued cDNA sequence. To determine the gene trap insertion site in *Sel1l*, we amplified the genomic fragment surrounding the gene trap insertion site using long-range PCR. Sequencing of the PCR products revealed that the gene trap cassette is located 79 base pairs upstream of exon 15 (Fig. 1*A*). The gene trap in *Sel1l* consists of a strong splicing acceptor site and a galactosidase-neomycin (βgeo) fusion gene and is expected to block splicing between exons 14 and 15. This will cause a truncation of wild-type SEL1L, resulting in a fusion protein containing the N-terminal 465 amino acids of SEL1L and βgeo (Fig. 1, *B* and *E*). PCR analysis of genomic DNAs from wild-type, heterozygous, and homozygous mutant embryos produced the expected band patterns, thus confirming the presence of the gene trap in *Sel1l* (Fig. 1*C*). RT-PCR analysis of RNAs from wild-type, heterozygous, and homozygous mutant embryos showed that the gene trap in *Sel1l* efficiently blocks RNA splicing between exons 14 and 15 (Fig. 1*D*), resulting in a truncated SEL1L and β-galactosidase fusion protein (Fig. 1*E*).

Heterozygous gene trap mice (*Sel1l*$^{+/-}$) appeared morphologically normal and were fertile. Of the 469 offspring obtained from intercrossing *Sel1l*$^{+/-}$ mice, no homozygous mutant (*Sel1l*$^{-/-}$) was found, suggesting that disruption of SEL1L function causes embryonic lethality (Fig. 1*F*). To determine at what developmental stage embryonic lethality occurs, we examined embryos from timed matings of *Sel1l*$^{+/-}$ mice. No live *Sel1l*$^{-/-}$ embryos were observed at E16.5 and only 2 (of 140) remained

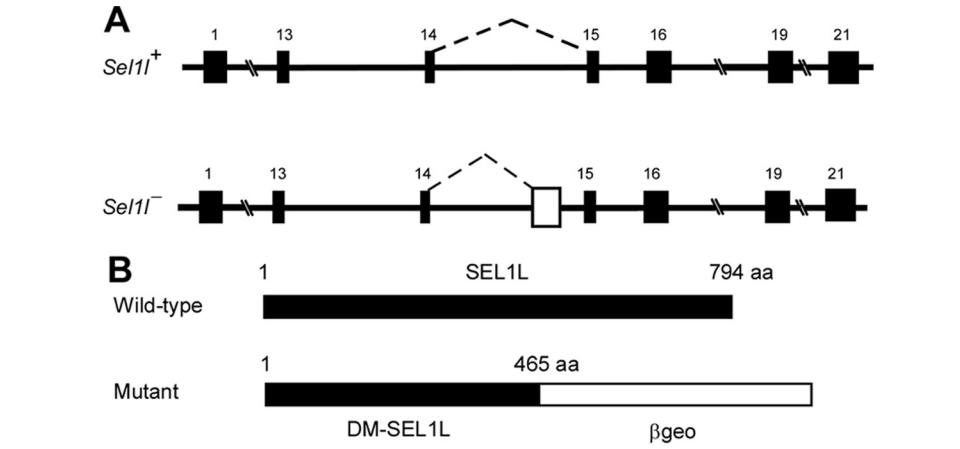

F

Genotype	E11.5	E12.5	E13.5	E14.5	E15.5	Weaning
Sel1l$^{+/+}$	56 (47)	52 (52)	20 (21)	52 (37)	42 (34)	145 (117)
Sel1l$^{+/-}$	107(97)	124 (104)	56 (42)	97 (75)	96 (69)	324 (234)
Sel1l$^{-/-}$	28 (47)	32 (52)	8 (21)	2 (37)	0 (34)	0 (117)
Total	191	208	84	151	138	469

G

FIGURE 1. **Generation and characterization of *Sel1l* gene trap mice.** *A*, schematic representation of wild-type (*Sel1l*$^{+}$) and gene-trapped (*Sel1l*$^{-}$) alleles in the *Sel1l* genomic locus. *Filled boxes* represent exons; the *open box* in *Sel1l*$^{-}$ indicates the trap cassette. *Dashed lines* indicate RNA splicing events. *B*, schematic representation of wild-type and DM-SEL1L peptides generated from *Sel1l*$^{+}$ and *Sel1l*$^{-}$ alleles, respectively. The number amino acids (*aa*) of each peptide is indicated. Note that the mutant peptide is a fusion protein containing the N-terminal 465 amino acids of SEL1L and βgeo. *C*, PCR analysis of genomic DNAs from *Sel1l*$^{+/+}$, *Sel1l*$^{+/-}$, and *Sel1l*$^{-/-}$ embryos at E11.5. *D*, RT-PCR analysis of RNAs from *Sel1l*$^{+/+}$, *Sel1l*$^{+/-}$, and *Sel1l*$^{-/-}$ embryos at E11.5. *Arrows* in *C* and *D* indicate PCR primers. *E*, Western blot analysis of wild-type and mutant SEL1L using anti-SEL1L and anti-β-galactosidase antibodies. Mutant SEL1L was detected as a 250-kDa SEL1L-β-geo fusion protein. *F*, distribution of *Sel1l*$^{+/+}$, *Sel1l*$^{+/-}$, and *Sel1l*$^{-/-}$ mice or embryos. *Numbers* in *parentheses* indicate expected distribution. *G*, representative images of *Sel1l*$^{+/+}$ (*right*) and *Sel1l*$^{-/-}$ (*left*) embryos. Note that the mutant embryo is markedly smaller than its wild-type littermate and its brain region is not properly formed.

alive at E15.5. The number of homozygous mutants obtained at E11.5 (28 of 191) was nearly 50% below the expected number (48), suggesting that some homozygous mutants were dead before E11.5. Nearly 95% of the homozygous mutant embryos at E12.5 were significantly smaller than their wild-type or heterozygous littermates. Half of the homozygous mutant embryos surviving to E13.5 showed morphological abnormality in the brain region (Fig. 1*G*).

Sel1l$^{-/-}$ *Embryos Develop Systemic Endoplasmic Reticulum Stress*—SEL1L is a homologue of the yeast protein Hrd3p, which has been implicated in protein quality control in the ER (32). To determine whether SEL1L deficiency leads to an impaired ER homeostasis and thereby ER stress in the developing embryo, we first compared the mRNA levels of 10 UPR genes between wild-type and mutant embryos using quantitative RT-PCR. These genes encode ER stress responsive transcription factors (Atf6, Chop, and Xbp1), ER chaperons (Herp, Edem1, Erdj3, Bip, p58IPK, and Ramp4), or ERAD component (Hrd1). Of the 10 genes, 7 were significantly up-regulated in the mutant embryos (Fig. 2*A*). Bip, Herp, and P58IPK, all encoding ER chaperons, showed 2.4-, 2.8-, and 2.5-fold increases, respectively, in mRNA levels in mutant embryos. The total Xbp1 mRNA level increased 1.7-fold in mutants and, importantly, the level of the spliced form of Xbp1 mRNA, which encodes the active form of XBP1, increased more than 2.5-fold. We speculated that SEL1L deficiency would lead to morphological changes of the ER. To test this, we compared the ultrastructure of the ER in wild-type and mutant hepatocytes using electron microscopy. Wild-type ER appeared thin or "relaxed" (Fig. 2*B*), whereas mutant ER appeared significantly dilated (Fig. 2*C*). Interestingly, fewer mitochondria were observed in mutant hepatocytes relative to wild-type controls. Similar morphological changes of the ER and mitochondria were observed in MEF from mutant embryos (data not shown). These results indicate that *Sel1l*$^{-/-}$ embryos develop systemic endoplasmic reticulum stress.

Increased Apoptosis in Mutant Embryos and Enhanced Cellular Sensitivity to ER Stress-inducing Reagents—ER stress has been shown to play a causal role in programmed cell death (43, 44). Therefore, we next investigated whether mutant embryos have increased apoptosis. Sections of E12.5 wild-type and mutant embryos were examined by TUNEL assay. Clear apoptotic signals were detected in the neural epithelium of the forebrain of mutant embryos, but not in the corresponding region of wild-type embryos (Fig. 3, *A* and *B*). Dorsal root ganglions of mutant embryos contained significantly more apoptotic cells than those of wild-type embryos (Fig. 3, *C* and *D*). These findings indicate that *Sel1l* function is critical for cell survival *in vivo*.

Primary MEF cells from *Sel1l*$^{-/-}$ embryos grew significantly slower relative to those from *Sel1l*$^{+/+}$ and *Sel1l*$^{+/-}$ embryos (supplemental Fig. S1). We speculated that this might be due to,

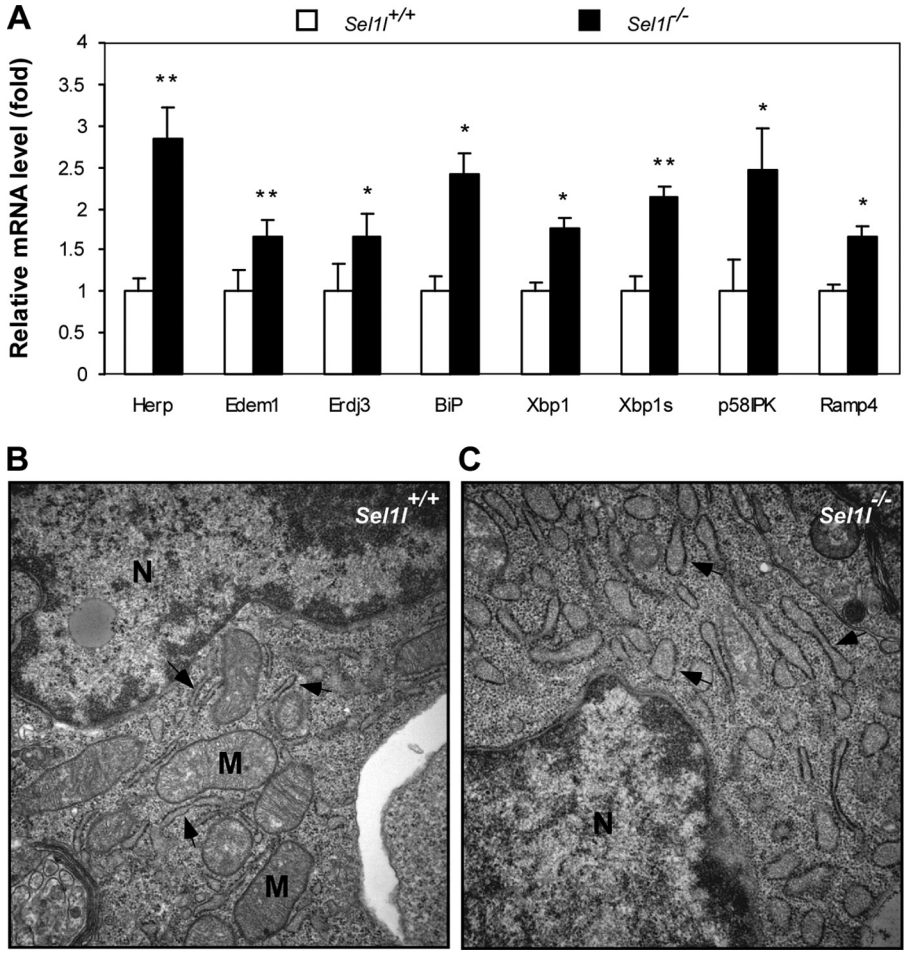

FIGURE 2. ***Sel1l*$^{-/-}$ embryos develop systemic endoplasmic reticulum stress.** *A*, quantitative analysis of ER stress-responsive genes in *Sel1l*$^{-/-}$ embryos. Total RNAs were isolated from *Sel1l*$^{+/+}$ and *Sel1l*$^{-/-}$ embryos at E12.5. The mRNA expression of several ER stress-inducible genes in *Sel1l*$^{+/+}$ and *Sel1l*$^{-/-}$ embryos was analyzed by quantitative RT-PCR. Data are expressed as expression-fold differences between *Sel1l*$^{+/+}$ (set to 1) and *Sel1l*$^{-/-}$ embryos. $n = 3$ embryos per genotype, *, $p < 0.05$; **, $p < 0.01$ mutant versus wild-type control. *B* and *C*, electron micrographs of liver sections from *Sel1l*$^{+/+}$ and *Sel1l*$^{-/-}$ embryos at E12.5. *Arrows* indicate endoplasmic reticulum; *N*, nucleus; *M*, mitochondria. Note that *Sel1l*$^{-/-}$ hepatocytes exhibit a significantly dilated ER (*arrows* in *C*) relative to those of *Sel1l*$^{+/+}$ hepatocytes (*arrows* in *B*).

at least partially, reduced cell viability of the mutant MEF. To assess this possibility, we stained equal numbers of wild-type and mutant MEFs with crystal violet. Mutant MEF showed a slightly lighter staining than wild-type MEF, an indication of reduced cell viability (Fig. 3*E*, 0 h TM treatment). We next investigated whether mutant MEF cells are more sensitive to ER stress-inducing reagents. Wild-type and mutant MEFs were treated for 1, 2, 3, and 4 h with 2 μM TM (an ER stress-inducing reagent) and then assayed for cell viability using crystal violet staining. TM treatment, whereas sharply reducing the viability of mutant MEF (>50% reduction after a 4-h TM treatment), only modestly affected that of wild-type MEF (<10% after a 4-h TM treatment) (Fig. 3, *E* and *F*). These results indicate that SEL1L deficiency predisposes embryonic cells to ER stress-inducing reagents.

To investigate the molecular basis underlying the hypersensitivity of mutant cells to ER stress-inducing reagents, we compared the intracellular level and phosphorylation of two ER stress signal sensors, PERK and IRE1a, in wild-type and mutant MEFs. Mutant MEFs contained significantly higher IRE1a than wild-type control MEFs (Fig. 3*G*, compare *lane 7* to *lane 1*). To assess the effect of SEL1L deficiency on ER stress signaling transduction, we treated wild-type and mutant MEFs with 75 nM thapsigargin (TG) for various durations and analyzed the treated cells by immunoblotting for IRE1a expression and PERK phosphorylation. As expected, TG treatment of wild-type MEFs induced a time-dependent increase of IRE1a levels and PERK phosphorylation (Fig. 3, *G*, *lanes 1*-6, and *H*, *lanes 1*-6, respectively). TG treatment slightly increased IRE1a levels (Fig. 3*G*, *lanes 7-13*) and induced normal PERK phosphorylation (Fig. 3, *G*, *lanes 7-13*, and *H*, *lanes 8-13*) in mutant MEFs. These data indicate that SEL1L deficiency does not compromise ER stress signaling transduction. The elevated intracellular levels of IRE1a and PERK may be responsible for the hypersensitivity of *Sel1l* mutant MEFs to ER stress-inducing reagents.

SEL1L-deficient MEF Cells Are Defective in ER-associated Degradation of Unfolded Proteins—SEL1L was thought to play a critical role in facilitating ERAD of unfolded/misfolded proteins (31, 45). To investigate whether the absence of SEL1L results in ERAD deficiency, we characterized the degradation of secretion-incompetent variant mutant human α_1-antitrypsin (also known as the null Hong-Kong mutation or NHK) in mutant MEF cells using a protein pulse-chase assay. This mutant α_1-antitrypsin was previously shown to be defective in folding into its functional conformation and was therefore targeted for degradation in the proteasomes (46). Immunoblotting showed that NHK was progressively degraded in wild-type MEFs. However, it was significantly stabilized in mutant MEFs (Fig. 4*A*). Quantification of NHK indicated that after 4 h of cycloheximide treatment (a potent protein synthesis inhibitor), as much as 90% of the transiently expressed NHK remained in mutant MEFs, whereas less than 20% of the transiently expressed NHK remained in wild-type MEFs (Fig. 4*D*). These observations indicate that disruption of SEL1L function severely compromises the ERAD function in mammalian cells.

To further assess the role of SEL1L in ERAD, we tested whether re-introduction of SEL1L could rescue the ERAD deficiency of mutant MEFs. NHK was transiently co-expressed in mutant MEFs with either full-length SEL1L or a deletion mutant that lacks the C-terminal 249 amino acids. In mutant MEFs co-expressing full-length SEL1L, NHK showed progres-

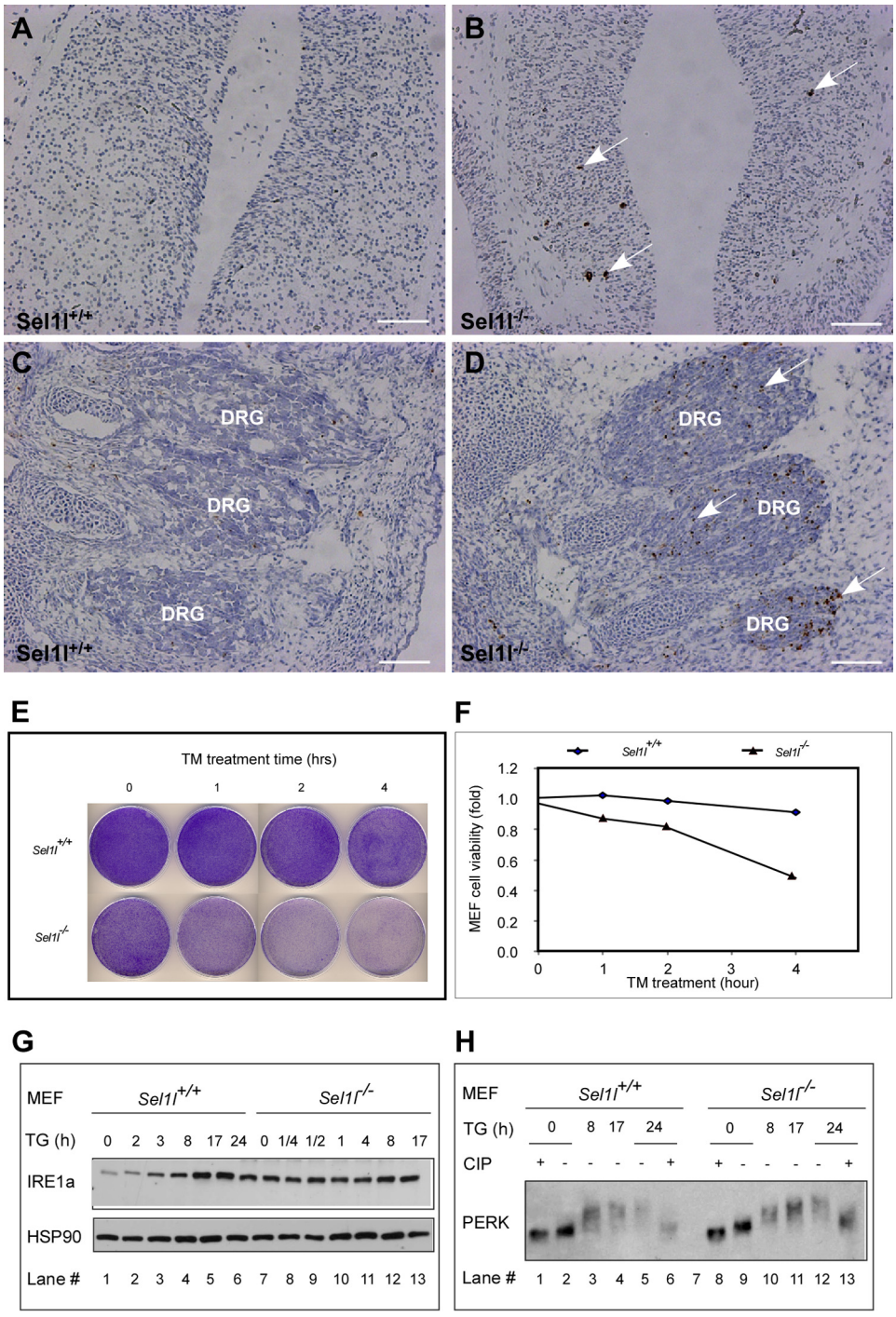

FIGURE 3. **SEL1L deficiency induces apoptosis *in vivo* and predisposes MEF cells to ER stress-inducing reagents.** *A–D*, increased apoptosis in *Sel1l*$^{-/-}$ embryos. Forebrain (*A* and *B*) and dorsal root ganglion (*DRG*) region sections (*C* and *D*) from *Sel1l*$^{+/+}$ and *Sel1l*$^{-/-}$ embryos at E12.5 were assayed by TUNEL. Apoptotic cells are indicated by *arrows*. *E*, representative images of crystal violet staining of tunicamycin-treated MEF cells. *Sel1l*$^{+/+}$ and *Sel1l*$^{-/-}$ MEF cells in 10-cm dishes were treated with 2 μg/ml of TM for the indicated periods, trypsinized, and re-plated (1×10^4 cells/per well) into 10-cm dishes. Five days later, the resulting cells were stained with crystal violet. *F*, quantification of MEF cell viabilities before and after TM treatment. Crystal violet-stained MEF cells in *E* were solubilized with 600 ml of 1% SDS, and absorbance of the resulting solution was measured at 570 nm. Relative cell viability was calculated as a percentage of absorbance of TM non-treated cells. *G*, Western blot analysis of IRE1a expression in *Sel1l*$^{+/+}$ and *Sel1l*$^{-/-}$ MEFs. *Sel1l*$^{+/+}$ and *Sel1l*$^{-/-}$ MEFs were treated with TG for the indicated periods. IRE1a and HSP90 (loading control) expression were analyzed by immunoblotting. Note that *Sel1l*$^{-/-}$ MEF has a noticeably higher basal level IRE1a expression than *Sel1l*$^{+/+}$ MEF (*lane 7 versus* 1). *H*, Western blot analysis of PERK phosphorylation. *Sel1l*$^{+/+}$ and *Sel1l*$^{-/-}$ MEFs were treated with TG for the indicated periods in the presence or absence of calf intestinal alkaline phosphatase (*CIP*). Lysates of the treated cells were blotted and probed with PERK antibody.

sive degradation; whereas in mutant MEFs co-expressing the truncated form of SEL1L, NHK was stabilized (Fig. 4*C*). Quantification of the transiently expressed NHK in both groups indicated that transient expression of SEL1L restored more than 90% of the ERAD capacity of mutant MEFs (Fig. 4*D*). These results verify that SEL1L function is essential for ERAD in mammalian cells. In addition, these data indicate that the C terminus of SEL1L contains important ERAD signals.

SEL1L-deficient Cells Have a Severely Impaired Protein Secretory Pathway—Blocking or a decrease of processing in the secretory pathway is a hallmark of ER stress in eukaryotic cells (47). To determine whether SEL1L deficiency blocks or impairs protein secretion, we compared the secretion of Gluc reporter, a naturally secreted protein (42), by wild-type and *Sel1l* mutant MEF cells. Wild-type and mutant MEFs were transiently transfected with an expression plasmid encoding Gluc. Conditioned medium of the transfected wild-type and mutant MEFs were collected at 12, 24, and 36 h post-transfection (hpt) and assayed for Gluc activity (Fig. 5*A*). Gluc activity was clearly detectable in the medium of both wild-type and mutant MEFs starting at 12 hpt. At this stage, the Gluc activity in wild-type MEF medium was 3.8-fold higher than that in the mutant MEF medium. Gluc activities in both wild-type and mutant MEF medium peaked around 24–36 hpt. The Gluc activity in wild-type MEF medium around this time was 9-fold higher than that in mutant MEF medium. We speculated that the majority of Gluc reporter protein might be retained within the mutant MEF cells. Therefore, we analyzed Gluc activity in the lysates of transfected wild-type and mutant MEFs at 24 hpt. Indeed, Gluc activity in the lysate of mutant MEFs was 9.4-fold higher than that in the lysate of wild-type MEFs (Fig. 5*B*). Altogether, these results indicate that SEL1L-deficient MEF cells have a severely impaired protein secretory pathway.

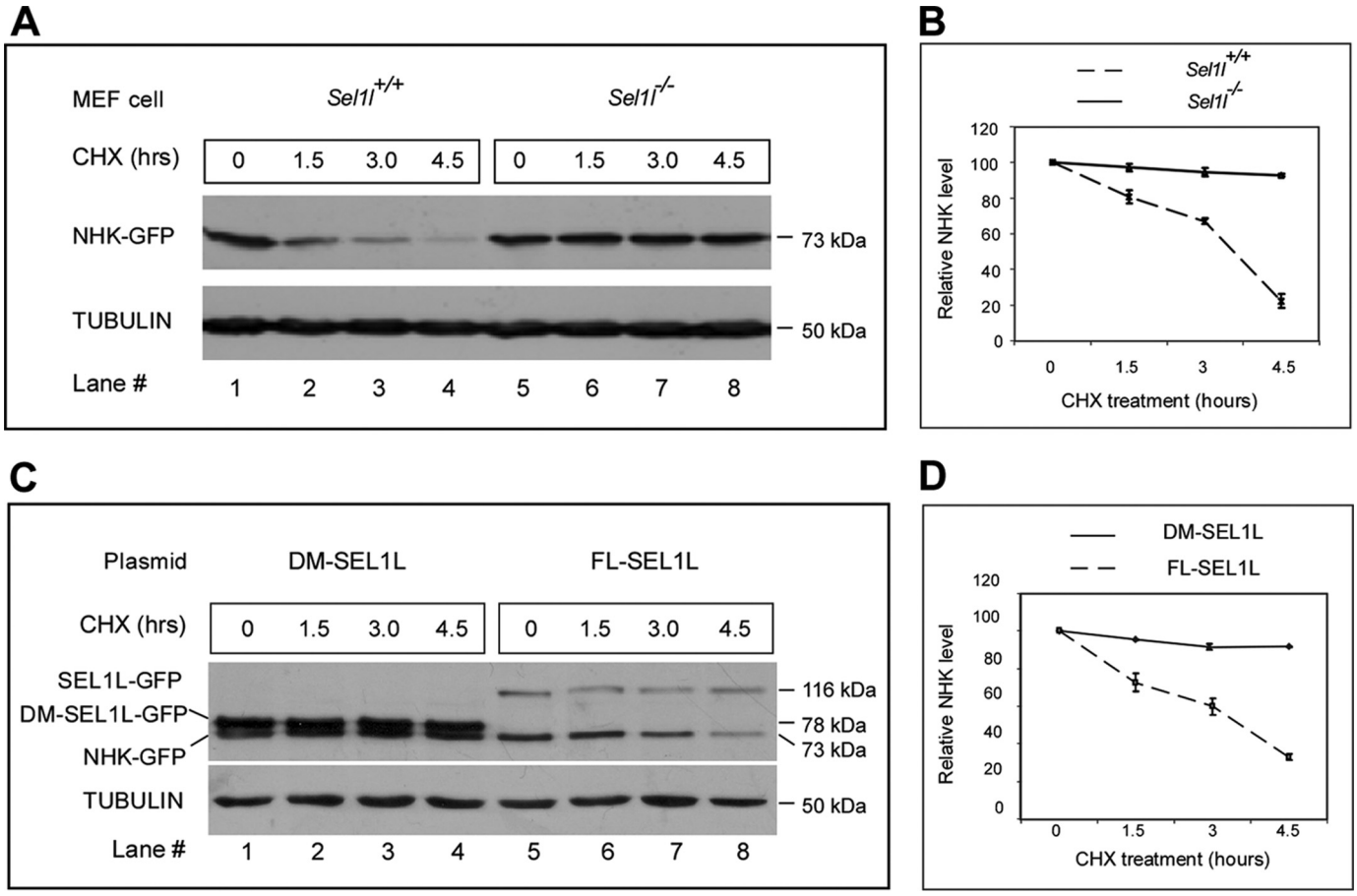

FIGURE 4. ***Sel1l*$^{-/-}$ MEF cells are defective in ER-associated protein degradation.** *A*, analysis of unfolded protein degradation in *Sel1l*$^{+/+}$ and *Sel1l*$^{-/-}$ MEFs. *Sel1l*$^{+/+}$ and *Sel1l*$^{-/-}$ MEFs were transfected with an expression plasmid encoding the GFP-tagged Hong Kong variant of mutant α_1-antitrypsin (NHK-GFP). NHK-GFP proteins in *Sel1l*$^{+/+}$ and *Sel1l*$^{-/-}$ MEF cells were pulse-chased for the indicated time and analyzed by Western blot analysis using a GFP antibody. The immunoblot was also probed with anti-tubulin antibody to ensure equal protein loading. *B*, quantification of NHK degradation rate in *A*. Relative NHK levels were calculated by dividing the normalized NHK signals in cells after 1.5, 3, and 4.5 h of cycloheximide (*CHX*) treatment with that of untreated cells. *C*, analysis of NHK degradation in *Sel1l*$^{-/-}$ MEF cells transiently expressing FL or a C-terminal DM-SEL1L. *Sel1l*$^{-/-}$ MEF cells were co-transfected with expression plasmids encoding NHK-GFP and FL-SEL1L-GFP or DM-SEL1L-GFP. Pulse-chase and immunoblot analyses were as described in *A*. SEL1L-GFP, DM-SEL1L-GFP, and NHK-GFP were detected as 116-, 78-, and 73-kDa protein products, respectively. *D*, quantification of NHK degradation rate in *Sel1l*$^{-/-}$ MEF cells co-expressing FL-SEL1L and DM-SEL1L. For all the NHK-GFP pulse-chase analyses, experiments were performed 3 times and the values were expressed as mean ± S.D.

Employing a similar technical approach, we next tested whether re-expression of full-length SEL1L could rescue the protein secretory defect in mutant MEF cells. Gaussia luciferase was transiently co-expressed in mutant MEF cells with either SEL1L-GFP or DM-SEL1L-GFP. Western blot analysis revealed that SEL1L-GFP and DM-SEL1L-GFP fusion proteins were expressed at a similar level in the mutant MEF (Fig. 5*C*). Gluc activity in the conditioned medium was analyzed at 24 and 36 hpt. Although expression of DM-SEL1L-GFP had no or little effect on the secretion of Gaussia luciferase protein in mutant MEFs, expression of SEL1L-GFP exhibited a remarkable rescuing effect on the secretion of the Gaussia luciferase reporter by mutant cells (Fig. 5*D*). We speculated that re-expression of SEL1L restores protein secretion rather than protein production in mutant MEF cells. To test this idea, we analyzed Gluc activity in the lysates of mutant MEFs transiently expressing SEL1L-GFP and DM-SEL1L-GFP. Indeed, the intracellular Gluc activity of SEL1L-expressing cells was 12- and 13-fold lower than that of Gluc alone and DM-SEL1L-expressing cells (Fig. 5*E*). Together, these results suggest that SEL1L functional deficiency causes blocking or dysfunction of the protein secretory pathway in mammalian cells.

The fact that transient expression of DM-SEL1L leads to a slight reduction of the Gaussia luciferase (Fig. 5*D*) indicates that DM-SEL1L may act as a dominant-negative SEL1L protein *in vitro* and *in vivo*. To test this possibility, we transiently expressed DM-SEL1L-GFP in HEK293 cells and assessed whether DM-SEL1L-GFP expression induces ER stress. Quantitative RT-PCR analysis revealed that the transcription of both Bip and Herp was significantly up-regulated in HEK293 cells expressing DM-SEL1L, as compared with HEK293 cells expressing GFP (Fig. 5*F*). This result suggests that ectopic expression of DM-SEL1L causes ER stress in HEK293 cells. Next, we transiently co-expressed Gaussia luciferase with DM-SEL1L-GFP in wild-type MEF cells and analyzed Gaussia luciferase activity in the conditioned medium at 12, 24, and 36 hpt. Co-expression of DM-SEL1L with Gaussia luciferase caused a drastic reduction of Gluc activity in the conditioned medium (Fig. 5*G*). These results are consistent with the hypothesis that DM-SEL1L functions as a dominant-negative protein. In addition, these results indicate that the C terminus of the SEL1L peptide contains important sequence elements essential for mediating the ERAD function in mammalian cells.

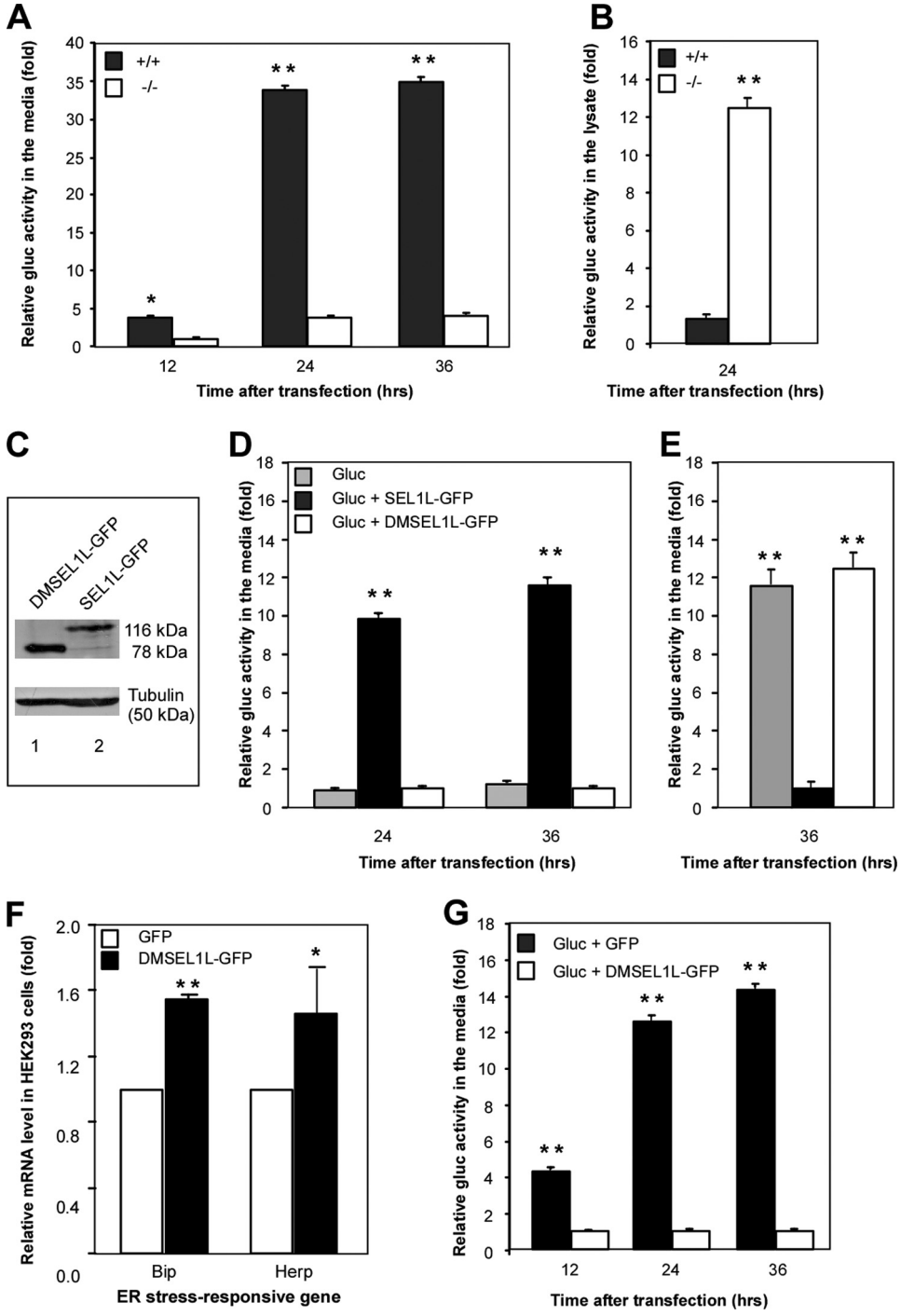

FIGURE 5. **Protein secretion is severely impaired in *Sel1l*$^{-/-}$ MEF cells.** *A* and *B*, rates of protein secretion by *Sel1l*$^{+/+}$ and *Sel1l*$^{-/-}$ MEF cells. *Sel1l*$^{+/+}$ and *Sel1l*$^{-/-}$ MEF cells were transfected with an expression plasmid encoding Gluc. Conditioned medium of the transfected cells were sampled at 12, 24, and 36 hpt and relative light units were measured by luciferase assay. The relative light units in the medium of *Sel1l*$^{-/-}$ MEF at 12 hpt was set to 1 and used to calculate relative Gluc activities (*A*). The Gluc-transfected *Sel1l*$^{+/+}$ and *Sel1l*$^{-/-}$ MEF cells were lysed at 24 hpt and their intracellular Gluc activities determined (*B*). *, $p < 0.05$; **, $p < 0.01$ wild-type *versus* mutant MEFs. *C*, Western blot analysis of SEL1L-GFP and DM-SEL1L-GFP expression in transfected *Sel1l*$^{-/-}$ MEF cells. The immunoblot was probed with anti-GFP and anti-tubulin antibodies. SEL1L-GFP, DM-SEL1L-GFP, and NHK-GFP were detected as 116- and 78-kDa protein products. *D*, rates of protein secretion by *Sel1l*$^{-/-}$ MEF transiently expressing SEL1L-GFP and DM-SEL1L-GFP. *Sel1l*$^{-/-}$ MEF cells were co-transfected with expression plasmids encoding Gluc and SEL1L-GFP or DM-SEL1L-GFP. Conditioned medium were sampled at 24 and 36 hpt and relative Gluc activities determined. *, $p < 0.05$; **, $p < 0.01$ Gluc + SEL1L-GFP/DM-SEL1L-GFP- *versus* Gluc-expressing cells. *E*, intracellular Gluc activities of the *Sel1l*$^{-/-}$ MEF cells in *D* at 36 hpt. *, $p < 0.05$; **, $p < 0.01$ Gluc or Gluc + DM-SEL1L-GFP- *versus* Gluc + SEL1L-GFP-expressing cells. *F*, quantitative RT-PCR analysis Bip and Herp mRNA expression in HEK293 cells transiently expressing GFP (control) and DM-SEL1L-GFP. *, $p < 0.05$; **, $p < 0.01$, DM-SEL1L-GFP- *versus* GFP-expressing HEK293 cells. *G*, rate of protein secretion by *Sel1l*$^{+/+}$ MEF transiently expressing DM-SEL1l. *Sel1l*$^{+/+}$ MEF cells were co-transfected with expression plasmids encoding Gluc and GFP or DM-SEL1L-GFP. Conditioned medium of the co-transfected cells were sampled at 12, 24, and 36 hpt and relative Gluc activities were measured. *, $p < 0.05$; **, $p < 0.01$ GFP- *versus* DM-SEL1L-GFP-expressing cells. Statistical analysis was based on data from three independent experiments.

DISCUSSION

We report that mice homozygous for a gene trap mutation in *Sel1l* die during mid-gestation with significantly elevated apoptosis in the developing brain, dorsal root ganglions, and liver. The ER in mutant hepatocytes is severely dilated. Mutant MEF cells exhibit growth retardation, increased sensitivity to ER stress-inducing reagents, defective degradation of unfolded proteins, and a severely blocked protein secretory pathway. Furthermore, genes encoding endoplasmic chaperone proteins and ERAD components are markedly up-regulated in homozygous mutant embryos. These data support the hypothesis that *Sel1l* regulates ER homeostasis during mouse embryonic development. To the best of our knowledge, this represents the first *in vivo* functional study for *Sel1l*.

Two lines of evidence strongly suggest that disruption of the *Sel1l* gene is responsible for the observed embryonic and cellular phenotypes. First, we have observed a consistent segregation of the observed embryonic phenotype with homozygosity for the gene trap insertion in *Sel1l* (Fig. 1). Second, we demonstrate convincingly *in vitro* that transient transfection of the full-length cDNA of *Sel1l* into mutant MEF cells rescues the defects in both unfolded protein degradation and protein secretion (see Figs. 4 and 5). However, it remains uncertain whether the homozygous gene trap mice are SEL1L null mutants. The gene trap *Sel1l* allele is predicted to generate a partial Sel1l peptide that lacks the carboxyl-terminal 329 amino acids. The truncated region contains several highly conserved motifs/domains that were shown to be critical for suppression of tumor cell growth (48). We have demonstrated that transient expression of the partial Sel1l peptide fails to rescue the ERAD and protein secretory defects in $Sel1l^{-/-}$ MEF cells (see Figs. 4 and 5). Nevertheless, it is possible the partial SEL1L peptide has other cellular function(s). Additionally, the mammalian *Sel1l* gene expresses multiple transcripts derived through alternative splicing among exons in the 5′ and 3′ ends of the gene (27). Indeed, our Northern analysis has detected at least two smaller transcripts in the mutant embryos. Thus, the mutant *Sel1l* allele may generate functional proteins. Further proof of this will require a detailed biochemical analysis of the Sel1l gene products in homozygous mutant embryos. Further studies are also needed to define the underlying cause(s) of the developmental failure of *Sel1l* mutant embryos.

Biochemical studies *in vitro* have shown that SEL1L is an ER membrane protein and is involved in the assembly of a multiprotein complex essential for retrotranslocation of unfolded/misfolded proteins from the ER lumen into the cytosol for proteasomal degradation (30, 32, 45). Consistent with this notion, we have provided three lines of evidence suggesting that SEL1L-deficient embryos develop systemic stress in the endoplasmic reticulum, most likely due to the functional failure of the ERAD system. First, a number of UPR response genes are significantly up-regulated in SEL1L-deficient embryos. These genes encode either ER chaperone proteins (Herp, Edem1, Erdj3, Bip, Hrd1, p58IPK, and Ramp4) or ERAD components (Hrd1 and Sel1l). The up-regulation of these UPR responsive genes is considered to be an essential adaptive mechanism to enhance the folding and degradation capacities of cells to temporarily cope with stress in the ER (15). Second, electron microscopy analysis shows that SEL1L-deficient MEF cells display a dilated ER. The change of ER morphology in Sel1l mutant cells is a clear indication that unfolded or misfolded proteins are accumulating, which is in line with SEL1L function in ERAD. Last, we demonstrate *in vitro* that SEL1L-deficient MEF cells have a greatly reduced ability to degrade NHK-GFP, a secretion-incompetent null variant of the human α_1-antitrypsin that contains a natural mutation that disrupts proper folding of the protein (46).

SEL1L facilitates ER-associated protein degradation by interacting with HRD1 (an E3 ubiquitin ligase) and several other ER membrane proteins (30, 45). In this regard, it is not surprising that the phenotype of the *Sel1l* gene trap mutant embryos shows similarity to that of the *Hrd1* (*Synoviolin*) knock-out mouse embryos. For instance, both *Hrd1* null and *Sel1l* gene trap mutant mice are embryonic lethal and develop systemic ER stress. It is noteworthy, however, that several clear differences exist between the two lines of mutant embryos. Over 95% of the *Sel1l* mutant embryos are growth retarded, but no growth retardation was reported for *Hrd1* null knock-out embryos. In addition, 80% of the *Sel1l* mutant embryos show morphological abnormality in the brain region, but the reported null Hrd1 knock-out embryos appear to be morphologically normal. The phenotypical differences of the *Sel1l* gene trap and *Hrd1* knock-out null mutant mice suggest that SEL1L may function in HRD1-dependent and HRD1-independent manners during mouse embryonic development. Further studies are needed to identify and characterize the HRD1-independent function(s) for SEL1L.

An intriguing question arising from our current study concerns the role(s) that *Sel1l* plays in adult mice. *Sel1l* is predominantly expressed in the islets and acinar cells of the pancreas (49, 50). Pancreatic islets secrete endocrine hormones into the bloodstream to regulate glucose homeostasis, while acinar cells produce hydrolytic enzymes for intestinal digestion. Given the highly secretory nature of the pancreatic cells, we speculate that SEL1L may be critically required for the functions and survival of pancreatic cells by maintaining their ER homeostasis.

In conclusion, we report a gene trap mouse mutation for *Sel1l*. Homozygous mutants are embryonic lethal and develop systemic endoplasmic reticulum stress. Mutant embryonic cells exhibit defective ER-associated degradation of unfolded proteins and have a severely impaired protein secretory pathway. Our data support a molecular model where SEL1L nucleates an ER membrane protein complex that facilitates ER homeostasis.

Acknowledgments—We thank Dr. Patrick Biggs (Wellcome Trust Sanger Institute, United Kingdom) for generously providing mouse ES cells containing the gene trap insertion in the Sel1l genomic locus and Drs. Yves Boisclair and Bruce Currie (Cornell University) for stimulating discussions and critical comments during preparation of the manuscript.

REFERENCES

1. Hammond, C., and Helenius, A. (1994) *J. Cell Biol.* **126,** 41–52
2. Ma, Y., and Hendershot, L. M. (2004) *J. Chem. Neuroanat.* **28,** 51–65

3. Gass, J. N., Gifford, N. M., and Brewer, J. W. (2002) *J. Biol. Chem.* **277,** 49047–49054
4. Lipson, K. L., Fonseca, S. G., Ishigaki, S., Nguyen, L. X., Foss, E., Bortell, R., Rossini, A. A., and Urano, F. (2006) *Cell Metab.* **4,** 245–254
5. Isler, J. A., Skalet, A. H., and Alwine, J. C. (2005) *J. Virol.* **79,** 6890–6899
6. Fels, D. R., and Koumenis, C. (2006) *Cancer Biol. Ther.* **5,** 723–728
7. Yacoub Wasef, S. Z., Robinson, K. A., Berkaw, M. N., and Buse, M. G. (2006) *Am. J. Physiol. Endocrinol. Metab.* **291,** E1274–E1280
8. Heazlewood, C. K., Cook, M. C., Eri, R., Price, G. R., Tauro, S. B., Taupin, D., Thornton, D. J., Png, C. W., Crockford, T. L., Cornall, R. J., Adams, R., Kato, M., Nelms, K. A., Hong, N. A., Florin, T. H., Goodnow, C. C., and McGuckin, M. A. (2008) *PLoS Med.* **5,** e54
9. Lee, J. W., Beebe, K., Nangle, L. A., Jang, J., Longo-Guess, C. M., Cook, S. A., Davisson, M. T., Sundberg, J. P., Schimmel, P., and Ackerman, S. L. (2006) *Nature* **443,** 50–55
10. Roybal, C. N., Marmorstein, L. Y., Vander Jagt, D. L., and Abcouwer, S. F. (2005) *Invest. Ophthalmol. Vis. Sci.* **46,** 3973–3979
11. Wang, J., Takeuchi, T., Tanaka, S., Kubo, S. K., Kayo, T., Lu, D., Takata, K., Koizumi, A., and Izumi, T. (1999) *J. Clin. Invest.* **103,** 27–37
12. Aridor, M. (2007) *Adv. Drug Deliv. Rev.* **59,** 759–781
13. Brodsky, J. L. (2007) *Biochem. J.* **404,** 353–363
14. Hampton, R. Y. (2002) *Curr. Opin. Cell Biol.* **14,** 476–482
15. Ron, D., and Walter, P. (2007) *Nat. Rev. Mol. Cell Biol.* **8,** 519–529
16. Ni, M., and Lee, A. S. (2007) *FEBS Lett.* **581,** 3641–3651
17. Li, J., and Lee, A. S. (2006) *Curr. Mol. Med.* **6,** 45–54
18. Urano, F., Bertolotti, A., and Ron, D. (2000) *J. Cell Sci.* **113,** 3697–3702
19. Yoshida, H., Matsui, T., Yamamoto, A., Okada, T., and Mori, K. (2001) *Cell* **107,** 881–891
20. Acosta-Alvear, D., Zhou, Y., Blais, A., Tsikitis, M., Lents, N. H., Arias, C., Lennon, C. J., Kluger, Y., and Dynlacht, B. D. (2007) *Mol. Cell* **27,** 53–66
21. Lee, A. H., Iwakoshi, N. N., and Glimcher, L. H. (2003) *Mol. Cell. Biol.* **23,** 7448–7459
22. Proud, C. G. (2005) *Semin. Cell Dev. Biol.* **16,** 3–12
23. Wek, R. C., Jiang, H. Y., and Anthony, T. G. (2006) *Biochem. Soc. Trans.* **34,** 7–11
24. Sommer, T., and Jarosch, E. (2002) *Dev. Cell* **3,** 1–2
25. Wu, J., Rutkowski, D. T., Dubois, M., Swathirajan, J., Saunders, T., Wang, J., Song, B., Yau, G. D., and Kaufman, R. J. (2007) *Dev. Cell* **13,** 351–364
26. Yamamoto, K., Sato, T., Matsui, T., Sato, M., Okada, T., Yoshida, H., Harada, A., and Mori, K. (2007) *Dev. Cell* **13,** 365–376
27. Biunno, I., Cattaneo, M., Orlandi, R., Canton, C., Biagiotti, L., Ferrero, S., Barberis, M., Pupa, S. M., Scarpa, A., and Ménard, S. (2006) *J. Cell. Physiol.* **208,** 23–38
28. Cattaneo, M., Otsu, M., Fagioli, C., Martino, S., Lotti, L. V., Sitia, R., and Biunno, I. (2008) *J. Cell. Physiol.* **215,** 794–802
29. Cormier, J. H., Tamura, T., Sunryd, J. C., and Hebert, D. N. (2009) *Mol. Cell* **34,** 627–633
30. Hosokawa, N., Wada, I., Nagasawa, K., Moriyama, T., Okawa, K., and Nagata, K. (2008) *J. Biol. Chem.* **283,** 20914–20924
31. Mueller, B., Klemm, E. J., Spooner, E., Claessen, J. H., and Ploegh, H. L. (2008) *Proc. Natl. Acad. Sci. U.S.A.* **105,** 12325–12330
32. Mueller, B., Lilley, B. N., and Ploegh, H. L. (2006) *J. Cell Biol.* **175,** 261–270
33. Oresic, K., Mueller, B., and Tortorella, D. (2009) *Biosci. Rep.* **29,** 173–181
34. Kaneko, M., Yasui, S., Niinuma, Y., Arai, K., Omura, T., Okuma, Y., and Nomura, Y. (2007) *FEBS Lett.* **581,** 5355–5360
35. Cattaneo, M., Lotti, L. V., Martino, S., Cardano, M., Orlandi, R., Mariani-Costantini, R., and Biunno, I. (2009) *J. Biol. Chem.* **284,** 11405–11415
36. Vandesompele, J., De Preter, K., Pattyn, F., Poppe, B., Van Roy, N., De Paepe, A., and Speleman, F. (2002) *Genome Biol.* **3,** RESEARCH0034
37. Orlandi, R., Cattaneo, M., Troglio, F., Campiglio, M., Biunno, I., and Ménard, S. (2002) *Int. J. Biol. Markers* **17,** 104–111
38. Zinszner, H., Kuroda, M., Wang, X., Batchvarova, N., Lightfoot, R. T., Remotti, H., Stevens, J. L., and Ron, D. (1998) *Genes Dev.* **12,** 982–995
39. Rutkowski, D. T., Arnold, S. M., Miller, C. N., Wu, J., Li, J., Gunnison, K. M., Mori, K., Sadighi Akha, A. A., Raden, D., and Kaufman, R. J. (2006) *PLoS Biol.* **4,** e374
40. Gardner, R. G., Swarbrick, G. M., Bays, N. W., Cronin, S. R., Wilhovsky, S., Seelig, L., Kim, C., and Hampton, R. Y. (2000) *J. Cell Biol.* **151,** 69–82
41. Sambrook, J., Fritsch, E. F., and Maniatis, T. (1989) *Molecular Cloning: A Laboratory Manual*, 2nd Ed., Cold Spring Harbor Laboratory, Cold Spring Harbor, NY
42. Badr, C. E., Hewett, J. W., Breakefield, X. O., and Tannous, B. A. (2007) *PLoS One* **2,** e571
43. Rao, R. V., Ellerby, H. M., and Bredesen, D. E. (2004) *Cell Death Differ.* **11,** 372–380
44. Rao, R. V., Niazi, K., Mollahan, P., Mao, X., Crippen, D., Poksay, K. S., Chen, S., and Bredesen, D. E. (2006) *Cell Death Differ.* **13,** 415–425
45. Christianson, J. C., Shaler, T. A., Tyler, R. E., and Kopito, R. R. (2008) *Nat. Cell Biol.* **10,** 272–282
46. Sifers, R. N., Brashears-Macatee, S., Kidd, V. J., Muensch, H., and Woo, S. L. (1988) *J. Biol. Chem.* **263,** 7330–7335
47. van Anken, E., and Braakman, I. (2005) *Crit. Rev. Biochem. Mol. Biol.* **40,** 269–283
48. Cattaneo, M., Canton, C., Albertini, A., and Biunno, I. (2004) *Gene* **326,** 149–156
49. Biunno, I., Appierto, V., Cattaneo, M., Leone, B. E., Balzano, G., Socci, C., Saccone, S., Letizia, A., Della Valle, G., and Sgaramella, V. (1997) *Genomics* **46,** 284–286
50. Donoviel, D. B., Donoviel, M. S., Fan, E., Hadjantonakis, A., and Bernstein, A. (1998) *Mech. Dev.* **78,** 203–207